

Ethylene Carbonylation to 3-Pentanone with In Situ Hydrogen via a Water–Gas Shift Reaction on Rh/CeO₂

Kun Zhang, Qiang Guo,* Yehong Wang, Pengfei Cao, Jian Zhang, Marc Heggen, Joachim Mayer, Rafal E. Dunin-Borkowski, and Feng Wang*



Cite This: *ACS Catal.* 2023, 13, 3164–3169



Read Online

ACCESS |



Metrics & More



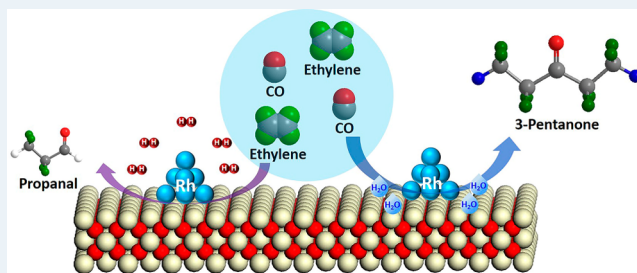
Article Recommendations



Supporting Information

ABSTRACT: Alkene carbonylation, in which hydrogenation plays pivotal roles, is one of the most efficient methods for the production of oxygenated chemicals like aldehydes, amides, and esters, among others. In this work, using in situ produced hydrogen via a water–gas shift (WGS) reaction, selective ethylene carbonylation to 3-pentanone was achieved instead of hydroformylation to propionaldehyde with gaseous H₂ on a defective ceria-supported Rh catalyst. The interface of Rh/CeO₂, which consists of oxygen vacancies and positively charged Rh, activates water, CO, and ethylene and the subsequent reactions, including the WGS reaction and ethylene carbonylation. The lean hydrogen circumstance created by the WGS reaction suppresses the hydrogenation of the propionyl group and promotes its ethylation to 3-pentanone. A redox pathway was proposed for the WGS reaction based on the in situ FTIR results, and the origin of hydrogen for ethylene carbonylation is water, as confirmed by a mass spectrometry (MS) study using d₂-water as one of the reactants. This work provides a promising method for heavier ketone synthesis.

KEYWORDS: cerium oxide, water–gas shift reaction, carbonylation, ketones, heterogeneous catalysis



Alkene carbonylation, in which two key steps are involved, namely, CO insertion and the sequential reaction of the acyl group,¹ is one of the most important methods for the production of value-added chemicals.^{1–5} The former step allows the addition of one carbonyl group to the carbon chain, and the latter one determines the nature of the products. For example, alcoholysis of the acyl group produces an ester,^{5,6} while hydrogenation of the acyl group produces an aldehyde, which is known as hydroformylation.² Insertion of CO followed by the creation of a C–C bond holds the promise to produce a ketone,^{7,8} which is another important family of organic compounds and widely used as solvents, polymer precursors, and pharmaceuticals.⁹ For instance, 3-pentanone is always used as a solvent in paint and as a precursor to vitamin E, and the current production of 3-pentanone from ethylene follows a two-step process involving ethylene hydroformylation to propanal, followed by propanal ketonization to 3-pentanone under oxidative conditions.^{10,11} Ethylene hydroformylation always generates 3-pentanone as one of the byproducts, which provides a potential route for the one-step synthesis of 3-pentanone if the main product of ethylene hydroformylation can be tuned toward 3-pentanone instead of propanal (Scheme S1).^{12,13} Recently, Sun et al. reported that, on a single-atom Ru catalyst, the selectivity of 3-pentanone in ethylene hydroformylation can be greatly improved due to the lower energy barrier of propionyl ethylation compared with that of propionyl hydrogenation.¹⁴ However, propionyl hydrogenation

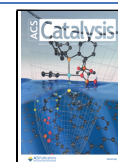
overwhelmingly dominates, which always produces propanal as the main product due to the surplus hydrogen on Rh catalysts under ethylene hydroformylation conditions (Scheme 1, routes 1-1 to 3-1). For example, Takahashi and co-workers discovered that Rh/active carbon was an effective catalyst for 3-pentanone production via ethylene hydroformylation, but it was still the minor product.¹⁵

In situ generated hydrogen, which is widely used for selective hydrogenation reactions,^{16,17} holds the promise to suppress propionyl hydrogenation and boost the ethylation of the propionyl group to 3-pentanone. Coupled with alcohol dehydrogenation–transfer hydrogenation, ethylene carbonylation to 3-pentanone was attained with the production of 1,1-diethoxyethane or acetone⁸ as the byproduct. The water–gas shift (WGS) reaction, in which water acts as a clean hydrogen source, is one of the most important processes for on-site hydrogen production. Ceria-supported metal catalysts show excellent performance for the WGS reaction due to their unique properties like the interfacial sites constructed by the ceria oxygen vacancy and the positively charged metal.^{18–21}

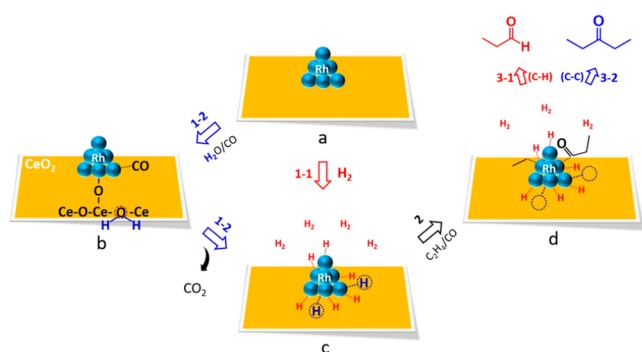
Received: December 12, 2022

Revised: February 8, 2023

Published: February 17, 2023



Scheme 1. Ethylene Carbonylation with H₂ (Red) or In Situ Produced H (Blue) via a Water–Gas Shift (WGS) Reaction on a Supported Rh Catalyst^a



^a(a) Supported Rh catalyst, (b) activation of CO and H₂O on Rh/CeO₂, (c) activated H on the supported Rh catalyst, and (d) key intermediates on the supported Rh catalyst.

Two different mechanisms, redox and formate processes, were proposed for the low-temperature WGS reaction on ceria-supported metal catalysts.^{18,20,22–24} For example, Gorte et al. proposed that metal-activated CO was oxidized by the lattice oxygen of ceria and the reduced ceria with oxygen vacancies, in turn, was oxidized by H₂O,²⁰ while Rodriguez et al. reported that formate, which decomposed to CO₂ and H₂, was the key intermediate.^{25,26} However, both mechanisms agree that CO and H₂O were, respectively, activated on the supported metal and oxygen vacancies of ceria (Scheme 1b), and it is well-known that alkene is activated on the supported metal, highlighting the crucial roles of the interface of ceria-supported metal catalysts.

In this work, using the in situ generated hydrogen via the WGS reaction, selective ethylene carbonylation to 3-pentanone was achieved on defective Rh/CeO₂ (Scheme 1, routes 1–2 to 3–2). CO and water were activated on positively charged Rh and oxygen vacancies, respectively, and the WGS reaction proceeded via a redox pathway, as the bicarbonate species were merely observed in the in situ FTIR spectra. A mass spectrometry study with *d*₂-water confirmed that the hydrogen source for ethylene carbonylation to 3-pentanone truly originated from water, and this route provides an alternative method for producing heavier ketones via alkene carbonylation.

In situ FTIR spectroscopy was first used to study the WGS reaction on Rh/CeO₂ at near-carbonylation reaction con-

ditions, and the in situ FTIR spectra collected are shown in Figure 1. Besides the bands at 2085 and 2015 cm⁻¹, which are attributed to the positively charged Rh carbonyl species, and the band at 2070 cm⁻¹, which is ascribed to the linear CO adsorbed on Rh⁰ (Figure 1a),²⁷ two bands at 2360 and 2340 cm⁻¹, which arise from CO₂, were also observed once the reaction was started at 160 °C (Figure 1b). Moreover, a broad band centered at 1616 cm⁻¹ appeared, which is assigned to the bicarbonate species, and other bands ranging from 1300 to 1500 cm⁻¹ are attributed to the carbonate species.^{28,29} With prolonged the reaction times, the band at 1616 cm⁻¹ first became stronger and then gradually weakened, which indicates that the bicarbonate species is a vital intermediate (Scheme S2). Meanwhile, the intensity of the bands at 2085 and 2015 cm⁻¹, which are from the positively charged Rh carbonyl species, decreased, while the band at 2070 cm⁻¹, which arises from the Rh⁰ carbonyl species, remained almost unchanged. In addition, the CO₂-related bands at 2360 and 2340 cm⁻¹ got stronger, while no band related to the formate was observed. The bands at 2085 and 2015 cm⁻¹ disappeared after 20 min of reaction and, concurrently, the band at 1616 cm⁻¹ started to weaken. This implies that the bicarbonate species was produced from CO adsorbed on the positively charged Rh. A new band at 1533 cm⁻¹, which is ascribed to the unidentate carbonates, was observed, and this band along with the carbonates bands at 1330, 1444, and 1480 cm⁻¹ became stronger when the reaction time was extended.³⁰ After evacuation, the gaseous CO₂ was removed, while the adsorbed species on the catalyst like the carbonates and Rh⁰ carbonyl species remained almost intact. These results demonstrate that the WGS reaction proceeds via a redox pathway in which the interfacial positively charged Rh activates CO and the bicarbonate species is generated as a key intermediate for the WGS reaction on Rh/CeO₂ at near-carbonylation conditions.

Rh/CeO₂ was then used for ethylene carbonylation with H₂ or in situ produced hydrogen via the WGS reaction. Propionaldehyde was produced as the major product; this process is well-known for hydroformylation when gaseous H₂ (0.5 MPa) is used as the hydrogen source (Figure 2a). The selectivity of 3-pentanone increased as the H₂ pressure decreased, and 60 mmol/mmol_{Rh} 3-pentanone was obtained at *t* = 4 h with a selectivity of 65% when 0.1 MPa H₂ was used. When H₂O was used as the sole hydrogen source via the WGS reaction, as expected, a high selectivity (92%) of 3-pentanone was achieved, although the lean hydrogen circumstance results in a lower yield of 3-pentanone (36 mmol/mmol_{Rh}) at *t* = 4 h. With a prolonged reaction time, the yield of 3-pentanone

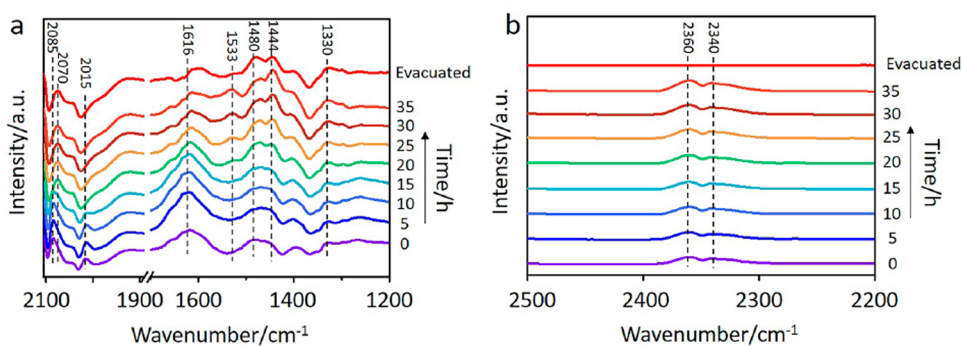


Figure 1. In situ FTIR spectra of the WGS reaction on Rh/CeO₂ (a) from 2100 to 1200 cm⁻¹ and (b) from 2500 to 2200 cm⁻¹.

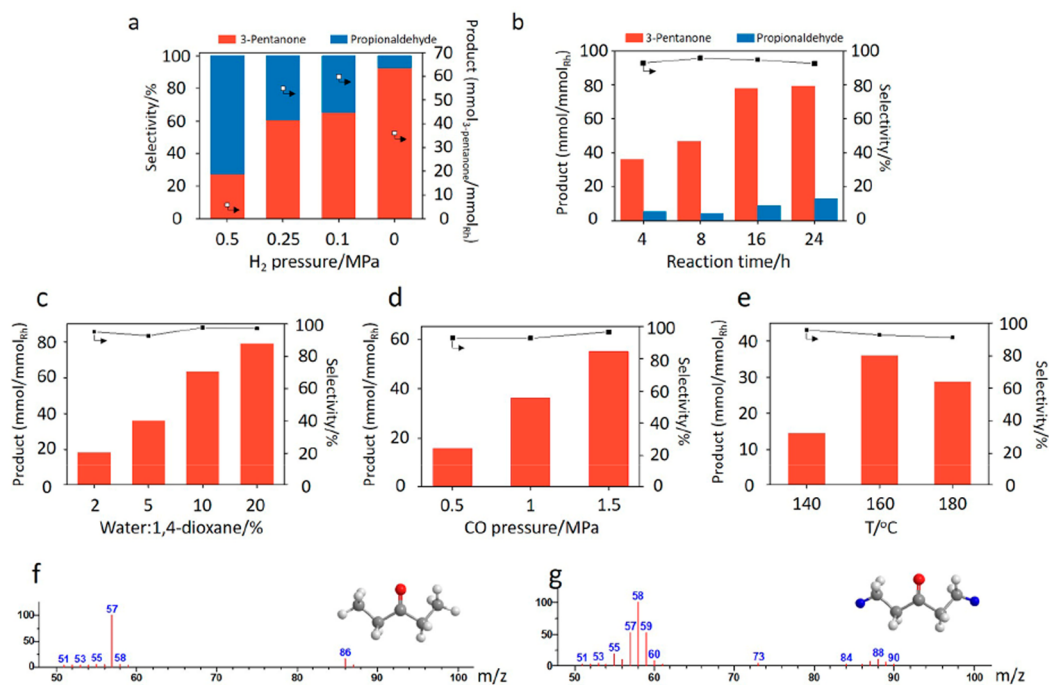


Figure 2. Ethylene carbonylation on Rh/CeO₂ at (a) different H₂ pressures, (b) various reaction times, (c) different water contents, (d) different CO pressures, and (e) different temperatures. Mass spectra of 3-pentanone produced from ethylene carbonylation with (f) H₂O and (g) D₂O; red = O, gray = C, white = H, and blue = D. Reaction conditions are as follows: 50 mg Rh/CeO₂, 3 mmol ethylene, 1.0 MPa CO (a, 1.0 MPa CO/H₂), 3 mL of 1,4-dioxane, 150 μ L of water, and 1 mmol *n*-dodecane as the internal standard at 160 °C for 4 h.

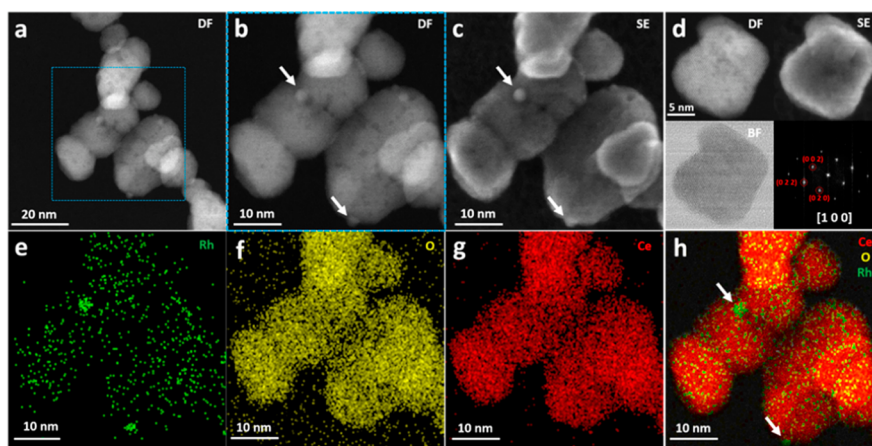


Figure 3. (a–d) Dark field (DF) and secondary electron (SE) STEM images. Corresponding EDX-STEM elemental mapping of (e) Rh, (f) O, and (g) Ce and (h) EDX-[Rh, O, Ce] of Rh/CeO₂.

increased with almost unchanged selectivity, and the 3-pentanone yield can reach 80 mmol/mmol_{Rh} with 13 mmol/mmol_{Rh} propionaldehyde at $t = 24$ h (Figure 2b). No carbonylation products were observed over bare CeO₂ (not shown for clarity), and only trace amounts of carbonylation products were produced on SiO₂- and TiO₂-supported Rh catalysts and ceria-supported Ru and Pt catalysts (Figure S1).

To confirm the participation of water and CO, various amounts of water and different CO pressures were used to study their effects on both the yield and selectivity of 3-pentanone (Figure 2c and d). A limited amount of 3-pentanone (18 mmol/mmol_{Rh}) was obtained when 2% water was used, although the selectivity was high (95%). As the water amount increased, the selectivity kept unchanged and the yield gradually increased. Up to 80 mmol_{3-pentanone}/mmol_{Rh} was

produced when 20% water was added (Figure 2c). In regular water, the molecular ion peak of 3-pentanone was $m/z = 86$ and the strongest ion peak was $m/z = 57$, which belongs to the fragment ion of CH₃CH₂CO⁻ (Figure 2f). When the water was replaced by D₂O, the molecular ion peak of 3-pentanone moved to $m/z = 88$ and $m/z = 58$ was the strongest ion peak, which could be assigned to the fragment ion of C(D)-H₂CH₂CO⁻ (Figure 2g). The isotopic tracing experiments confirmed that the H for ethylene carbonylation originated from water and located at the C(1) and C(5) sites of 3-pentanone and the C(1) and C(3) sites of propionaldehyde, which was produced by ethylene hydroformylation as the byproduct (Figure S2). Increasing the CO pressure also boosted the production of 3-pentanone, and the yield of 3-pentanone was increased from 15 to 55 mmol/mmol_{Rh} when

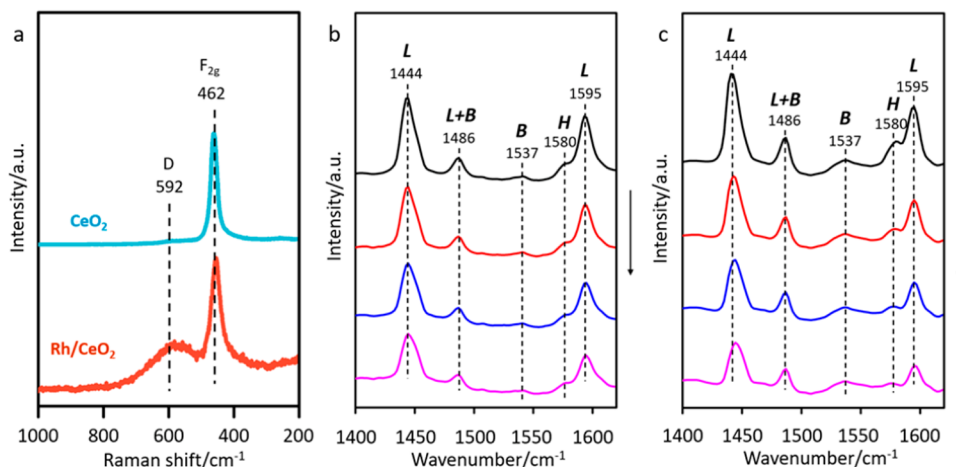


Figure 4. (a) Raman spectra of Rh/CeO₂ and CeO₂ excited at 532 nm. FTIR spectra after pyridine adsorption and evacuation in vacuo on Rh/CeO₂ (b) before and (c) after water adsorption (the arrow indicates the desorbing sequence of pyridine in vacuo).

1.5 MPa CO was charged into the reactor instead of 0.5 MPa (Figure 2d). The effect of temperature was also studied, and it was found that the highest yield of 3-pentanone (36 mmol/mmol_{Rh}) was obtained when the reaction was done at 160 °C (Figure 2e). This should come from the fact that the elimination reaction on Rh, which is an exothermic reaction, is unfavorable at higher temperatures. The stability of the catalyst was also studied, and the activity of Rh/CeO₂ decreased in the second run, with unchanged selectivity (Figure S3a). The IR spectrum of CO adsorption on the used catalyst indicates that Rh aggregated during the reaction, which lowered the activity of the catalyst (Figure S3b).

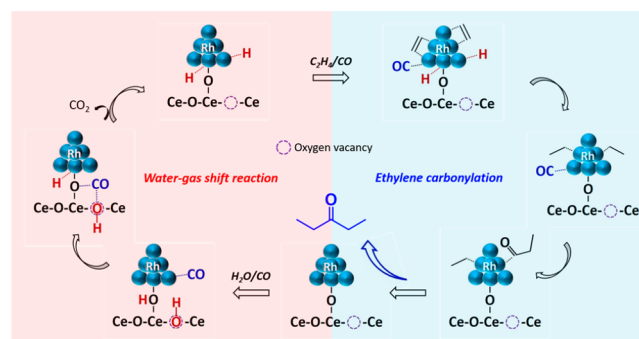
Figure 3a–d show high-angle annular dark-field (HAADF) scanning transmission electron microscopy (STEM) images of Rh/CeO₂, and corresponding spatially resolved energy-dispersive X-ray (EDX) maps of Rh/CeO₂ are exhibited in Figure 3e–h. STEM images show that the ceria particle size is about 10 nm and a few small Rh nanoparticles (about 2 nm in diameter) are located on the ceria. Highly dispersed Rh species with trace amounts of small Rh nanoparticles were also revealed by EDX mapping of Rh/CeO₂, and this is in accordance with the FTIR study that indicates that both positively charged and metallic Rh are present on ceria (Figures S4 and S5).

Raman spectra of Rh/CeO₂ and bare CeO₂ are shown in Figure 4a. Two characteristic Raman bands at 592 and 462 cm⁻¹, which are assigned to the defect-induced mode and the F_{2g} mode of CeO₂, respectively,^{31,32} were observed. The relative intensity ratio of I_{592}/I_{462} was significantly enhanced after Rh was supported on ceria. This comes from the fact that metal–support interactions between Rh and ceria greatly promote interfacial oxygen vacancy formation via $\text{Rh}^{\delta+}-\text{O}-\text{Ce}-\text{Ov}-\text{Ce}$.^{8,33,34} When ethylene was adsorbed on the Rh/CeO₂, three IR bands at 2875, 2940, and 2960 cm⁻¹ appeared, which were assigned to the di- σ -bonded ethylene, and this indicates that ethylene mainly adsorbed on the highly dispersed Rh clusters or nanoparticles (Figure S6). Figure 4b and c show the IR spectra of adsorbed pyridine on Rh/CeO₂ before and after water adsorption, respectively. In addition to the bands attributed to Lewis acid sites (1444, 1486, and 1595 cm⁻¹), only a faint peak at 1537 cm⁻¹, which was assigned to the pyridine adsorbed on Brønsted acid sites, and a weak shoulder peak at 1580 cm⁻¹ corresponding to H-bonded

pyridine were observed on Rh/CeO₂ without water preadsorption.^{35,36} After water was preadsorbed on the Rh/CeO₂ catalyst, the peaks at 1537 and 1580 cm⁻¹ became stronger. However, no pyridine adsorbed on Brønsted acid sites was observed when water was preadsorbed on pure CeO₂ (Figure S7). This indicates that the interfacial oxygen vacancies of Rh/CeO₂ promote the dissociative adsorption of water.

Based on our results, we proposed the following pathway for ethylene carbonylation to 3-pentanone with in situ produced H via the WGS reaction on defective Rh/CeO₂ (Scheme 2):

Scheme 2. Proposed Mechanism of Ethylene Carbonylation Coupled with a Water–Gas Shift Reaction to 3-Pentanone on Defective Rh/CeO₂



First, water was dissociatively adsorbed on the oxygen vacancy of ceria, while CO and ethylene were activated on Rh. The CO on positively charged Rh reacted with the hydroxyl groups produced from water to generate bicarbonate species. Then, the bicarbonate species decomposed: H was transferred onto the Rh surface, and the oxygen vacancy of ceria was restored when CO₂ was released from the ceria surface. The in situ generated H on Rh was preferentially captured by the activated ethylene to form an ethyl group, and then propionyl group was formed after CO insertion. The reaction of the propionyl group, which was always regarded as the rate-limiting step, determines the nature of the final products. Due to the lean H circumstance created by the WGS reaction on the Rh surface, hydrogenation of the propionyl group was deterred and ethylation of the propionyl group with another ethyl group on Rh to produce 3-pentanone was promoted. When gaseous H₂

was used as the H source, the Rh surface would be covered by surplus H due to the highly favorable activation of H₂ on Rh and the propionyl group would be hydrogenated to propionaldehyde.

In conclusion, coupled with the water–gas shift (WGS) reaction, highly selective ethylene carbonylation to 3-pentanone was achieved on a defective ceria-supported Rh catalyst. Water, which donates the hydrogen for ethylene carbonylation as confirmed by the MS study, is dissociated on the oxygen vacancies of ceria, CO is activated on positively charged Rh, and the subsequent steps for the WGS reaction proceed via a redox mechanism, as revealed by the in situ FTIR study. When gaseous H₂ was involved, the selectivity of 3-pentanone decreased due to the parallel reaction of ethylene hydroformylation, which underlines the key role of lean hydrogen produced via the WGS reaction for selective hydrogenation. This work opens an alternative route for heavier ketone synthesis.

■ ASSOCIATED CONTENT

SI Supporting Information

The Supporting Information is available free of charge at <https://pubs.acs.org/doi/10.1021/acscatal.2c06123>.

(PDF)

■ AUTHOR INFORMATION

Corresponding Authors

Qiang Guo – State Key Laboratory of Catalysis, Dalian National Laboratory for Clean Energy, Dalian Institute of Chemical Physics, Chinese Academy of Sciences, Dalian, Liaoning 116023, China; Email: qguo@dicp.ac.cn

Feng Wang – Henan Institute of Advanced Technology, Zhengzhou University, Zhengzhou, Henan 450003, China; State Key Laboratory of Catalysis, Dalian National Laboratory for Clean Energy, Dalian Institute of Chemical Physics, Chinese Academy of Sciences, Dalian, Liaoning 116023, China; orcid.org/0000-0002-9167-8743; Email: wangfeng@dicp.ac.cn

Authors

Kun Zhang – Henan Institute of Advanced Technology, Zhengzhou University, Zhengzhou, Henan 450003, China; State Key Laboratory of Catalysis, Dalian National Laboratory for Clean Energy, Dalian Institute of Chemical Physics, Chinese Academy of Sciences, Dalian, Liaoning 116023, China

Yehong Wang – State Key Laboratory of Catalysis, Dalian National Laboratory for Clean Energy, Dalian Institute of Chemical Physics, Chinese Academy of Sciences, Dalian, Liaoning 116023, China; orcid.org/0000-0002-2403-9976

Pengfei Cao – Ernst Ruska Centre for Microscopy and Spectroscopy with Electrons, Forschungszentrum Juelich GmbH, Juelich 52425, Germany; Central Facility for Electron Microscopy, RWTH Aachen University, 52074 Aachen, Germany

Jian Zhang – State Key Laboratory of Catalysis, Dalian National Laboratory for Clean Energy, Dalian Institute of Chemical Physics, Chinese Academy of Sciences, Dalian, Liaoning 116023, China

Marc Heggen – Ernst Ruska Centre for Microscopy and Spectroscopy with Electrons, Forschungszentrum Juelich GmbH, Juelich 52425, Germany

Joachim Mayer – Ernst Ruska Centre for Microscopy and Spectroscopy with Electrons, Forschungszentrum Juelich GmbH, Juelich 52425, Germany; Central Facility for Electron Microscopy, RWTH Aachen University, 52074 Aachen, Germany

Rafal E. Dunin-Borkowski – Ernst Ruska Centre for Microscopy and Spectroscopy with Electrons, Forschungszentrum Juelich GmbH, Juelich 52425, Germany; orcid.org/0000-0001-8082-0647

Complete contact information is available at: <https://pubs.acs.org/doi/10.1021/acscatal.2c06123>

Author Contributions

The manuscript was written through contributions of all authors. All authors have given approval to the final version of the manuscript.

Notes

The authors declare no competing financial interest.

■ ACKNOWLEDGMENTS

This work was supported by the National Natural Science Foundation of China (22172158, 21721004, and 22025206), the Sino-German Mobility Programme (M0304), the Department of Science and Technology of Dalian under the contract 2020RQ026, the Dalian Innovation Support Plan for High Level Talents (2020RT10), the Fundamental Research Funds for the Central Universities (20720220008), and the K. C. Wong Education Foundation of Chinese Academy of Sciences (GJTD-2020-08).

■ REFERENCES

- (1) Peng, J. B.; Geng, H. Q.; Wu, X. F. The Chemistry of CO: Carbonylation. *Chem.* **2019**, *5*, 526–552.
- (2) Franke, R.; Selent, D.; Borner, A. Applied Hydroformylation. *Chem. Rev.* **2012**, *112*, 5675–5732.
- (3) Kiss, G. Palladium-catalyzed Reppe carbonylation. *Chem. Rev.* **2001**, *101*, 3435–3456.
- (4) Wu, X. F.; Neumann, H.; Beller, M. Synthesis of Heterocycles via Palladium-Catalyzed Carbonylations. *Chem. Rev.* **2013**, *113*, 1–35.
- (5) Yang, J.; Liu, J. W.; Neumann, H.; Franke, R.; Jackstell, R.; Beller, M. Direct synthesis of adipic acid esters via palladium-catalyzed carbonylation of 1,3-dienes. *Science* **2019**, *366*, 1514–1517.
- (6) An, J. H.; Wang, Y. H.; Lu, J. M.; Zhang, J.; Zhang, Z. X.; Xu, S. T.; Liu, X. Y.; Zhang, T.; Gocyla, M.; Heggen, M.; Dunin-Borkowski, R. E.; Fornasiero, P.; Wang, F. Acid-Promoter-Free Ethylene Methoxycarbonylation over Ru-Clusters/Ceria: The Catalysis of Interfacial Lewis Acid-Base Pair. *J. Am. Chem. Soc.* **2018**, *140*, 4172–4181.
- (7) Wu, F. P.; Yuan, Y.; Liu, J. W.; Wu, X. F. Pd/Cu-Catalyzed Defluorinative Carbonylative Coupling of Aryl Iodides and gem-Difluoroalkenes: Efficient Synthesis of alpha-Fluoroaldehydes. *Angew. Chem., Int. Ed.* **2021**, *60*, 8818–8822.
- (8) Guo, Q.; Wang, Y. H.; Han, J. Y.; Zhang, J.; Wang, F. Interfacial Tandem Catalysis for Ethylene Carbonylation and C-C Coupling to 3-Pentanone on Rh/Ceria. *ACS Catal.* **2022**, *12*, 3286–3290.
- (9) Chalotra, N.; Sultan, S.; Shah, B. A. Recent Advances in Photoredox Methods for Ketone Synthesis. *Asian J. Org. Chem.* **2020**, *9*, 863–881.
- (10) Renz, M. Ketonization of carboxylic acids by decarboxylation: Mechanism and scope. *Eur. J. Org. Chem.* **2005**, *2005*, 979–988.

- (11) Kamimura, Y.; Sato, S.; Takahashi, R.; Sodesawa, T.; Fukui, M. Vapor-phase synthesis of symmetric ketone from alcohol over $\text{CeO}_2\text{-Fe}_2\text{O}_3$ catalysts. *Chem. Lett.* **2000**, *29*, 232–233.
- (12) Gorbunov, D. N.; Nenashcheva, M. V.; Matsukevich, R. P.; Terenina, M. V.; Putilin, F. N.; Kardasheva, Y. S.; Maksimov, A. L.; Karakhanov, E. A. Ethylene Hydroformylation in the Presence of Rhodium Catalysts in Hydrocarbon-Rich Media: The Stage of Combined Conversion of Refinery Gases to Oxygenates. *Petrol. Chem.* **2019**, *59*, 1009–1016.
- (13) Song, X. G.; Ding, Y. J.; Chen, W. M.; Dong, W. D.; Pei, Y. P.; Zang, J.; Yan, L.; Lu, Y. Formation of 3-pentanone via ethylene hydroformylation over Co/activated carbon catalyst. *Appl. Catal. A-Gen.* **2013**, *452*, 155–162.
- (14) Qin, T. T.; Dang, Y. R.; Lin, T. J.; Mei, B. B.; Wu, B.; Li, X.; Li, S. G.; Jiang, Z.; Tang, Z. Y.; Zhong, L. S.; Sun, Y. H. Single-atom Ru catalyst for selective synthesis of 3-pentanone via ethylene hydroformylation. *Green Chem.* **2021**, *23*, 9038–9047.
- (15) Takahashi, N.; Takeyama, T.; Yanagibashi, T.; Takada, Y. Comparison of Pentan-3-One Formation with Propionaldehyde Formation during Ethylene Hydroformylation over Rh Active-Carbon Catalyst. *J. Catal.* **1992**, *136*, 531–538.
- (16) Hao, C. H.; Guo, X. N.; Pan, Y. T.; Chen, S.; Jiao, Z. F.; Yang, H.; Guo, X. Y. Visible-Light-Driven Selective Photocatalytic Hydrogenation of Cinnamaldehyde over Au/SiC Catalysts. *J. Am. Chem. Soc.* **2016**, *138*, 9361–9364.
- (17) He, L.; Yu, F. J.; Lou, X. B.; Cao, Y.; He, H. Y.; Fan, K. N. A novel gold-catalyzed chemoselective reduction of α,β -unsaturated aldehydes using CO and H_2O as the hydrogen source. *Chem. Commun.* **2010**, *46*, 1553–1555.
- (18) Montini, T.; Melchionna, M.; Monai, M.; Fornasiero, P. Fundamentals and Catalytic Applications of CeO_2 -Based Materials. *Chem. Rev.* **2016**, *116*, 5987–6041.
- (19) Rodriguez, J. A.; Grinter, D. C.; Liu, Z. Y.; Palomino, R. M.; Senanayake, S. D. Ceria-based model catalysts: fundamental studies on the importance of the metal-ceria interface in CO oxidation, the water-gas shift, CO_2 hydrogenation, and methane and alcohol reforming. *Chem. Soc. Rev.* **2017**, *46*, 1824–1841.
- (20) Bunluesin, T.; Gorte, R. J.; Graham, G. W. Studies of the water-gas-shift reaction on ceria-supported Pt, Pd, and Rh: implications for oxygen-storage properties. *Appl. Catal., B* **1998**, *15*, 107–114.
- (21) Vecchietti, J.; Bonivardi, A.; Xu, W. Q.; Stacchiola, D.; Delgado, J. J.; Calatayud, M.; Collins, S. E. Understanding the Role of Oxygen Vacancies in the Water Gas Shift Reaction on Ceria-Supported Platinum Catalysts. *ACS Catal.* **2014**, *4*, 2088–2096.
- (22) Li, Y.; Fu, Q.; Flytzani-Stephanopoulos, M. Low-temperature water-gas shift reaction over Cu- and Ni-loaded cerium oxide catalysts. *Appl. Catal., B* **2000**, *27*, 179–191.
- (23) Shido, T.; Iwasawa, Y. Regulation of Reaction Intermediate by Reactant in the Water Gas Shift Reaction on CeO_2 , in Relation to Reactant-Promoted Mechanism. *J. Catal.* **1992**, *136*, 493–503.
- (24) Shido, T.; Iwasawa, Y. Reactant-Promoted Reaction-Mechanism for Water Gas Shift Reaction on Rh-Doped CeO_2 . *J. Catal.* **1993**, *141*, 71–81.
- (25) Rodriguez, J. A.; Ma, S.; Liu, P.; Hrbek, J.; Evans, J.; Perez, M. Activity of CeO_x and TiO_x nanoparticles grown on Au(111) in the water-gas shift reaction. *Science* **2007**, *318*, 1757–1760.
- (26) Rodriguez, J. A.; Liu, P.; Hrbek, J.; Evans, J.; Perez, M. Water gas shift reaction on Cu and Au nanoparticles supported on $\text{CeO}_2(111)$ and $\text{ZnO}(0001)$: Intrinsic activity and importance of support interactions. *Angew. Chem., Int. Ed.* **2007**, *46*, 1329–1332.
- (27) Lang, R.; Li, T. B.; Matsumura, D.; Miao, S.; Ren, Y. J.; Cui, Y. T.; Tan, Y.; Qiao, B. T.; Li, L.; Wang, A. Q.; Wang, X. D.; Zhang, T. Hydroformylation of Olefins by a Rhodium Single-Atom Catalyst with Activity Comparable to $\text{RhCl}(\text{PPh}_3)_3$. *Angew. Chem., Int. Ed.* **2016**, *55*, 16054–16058.
- (28) Wang, X. Q.; Rodriguez, J. A.; Hanson, J. C.; Gamarra, D.; Martinez-Arias, A.; Fernandez-Garcia, M. In situ studies of the active sites for the water gas shift reaction over Cu- CeO_2 catalysts: Complex interaction between metallic copper and oxygen vacancies of ceria. *J. Phys. Chem. B* **2006**, *110*, 428–434.
- (29) Garand, E.; Wende, T.; Goebbert, D. J.; Bergmann, R.; Meijer, G.; Neumark, D. M.; Asmis, K. R. Infrared Spectroscopy of Hydrated Bicarbonate Anion Clusters: $\text{HCO}_3^- (\text{H}_2\text{O})_{1-10}$. *J. Am. Chem. Soc.* **2010**, *132*, 849–856.
- (30) Coenen, K.; Gallucci, F.; Mezari, B.; Hensen, E.; van Sint Annaland, M. An in-situ IR study on the adsorption of CO_2 and H_2O on hydrotalcites. *J. CO₂ Util.* **2018**, *24*, 228–239.
- (31) Taniguchi, T.; Watanabe, T.; Sugiyama, N.; Subramani, A. K.; Wagata, H.; Matsushita, N.; Yoshimura, M. Identifying Defects in Ceria-Based Nanocrystals by UV Resonance Raman Spectroscopy. *J. Phys. Chem. C* **2009**, *113*, 19789–19793.
- (32) Wu, Z. L.; Li, M. J.; Howe, J.; Meyer, H. M.; Overbury, S. H. Probing Defect Sites on CeO_2 Nanocrystals with Well-Defined Surface Planes by Raman Spectroscopy and O_2 Adsorption. *Langmuir* **2010**, *26*, 16595–16606.
- (33) Acerbi, N.; Tsang, S. C. E.; Jones, G.; Golunski, S.; Collier, P. Rationalization of Interactions in Precious Metal/Ceria Catalysts Using the d-Band Center Model. *Angew. Chem., Int. Ed.* **2013**, *52*, 7737–7741.
- (34) Mao, M. Y.; Lv, H. Q.; Li, Y. Z.; Yang, Y.; Zeng, M.; Li, N.; Zhao, X. J. Metal Support Interaction in Pt Nanoparticles Partially Confined in the Mesopores of Microsized Mesoporous CeO_2 for Highly Efficient Purification of Volatile Organic Compounds. *ACS Catal.* **2016**, *6*, 418–427.
- (35) Parry, E. P. An Infrared Study of Pyridine Adsorbed on Acidic Solids Characterization of Surface Acidity. *J. Catal.* **1963**, *2*, 371–379.
- (36) Wu, Z. L.; Mann, A. K. P.; Li, M. J.; Overbury, S. H. Spectroscopic Investigation of Surface-Dependent Acid Base Property of Ceria Nanoshapes. *J. Phys. Chem. C* **2015**, *119*, 7340–7350.